



Free-water imaging of the hippocampus is a sensitive marker of Alzheimer's disease

Edward Ofori^{a,j,*}, Steven T. DeKosky^b, Marcelo Febo^{c,d}, Luis Colon-Perez^c, Paramita Chakrabarty^{d,e}, Ranjan Duara^f, Malek Adjouadi^g, Todd E. Golde^{d,e}, David E. Vaillancourt^{a,h,i}, for the Alzheimer's Disease Neuroimaging Initiative¹

^a Department of Applied Physiology and Kinesiology, University of Florida, Gainesville FL 32611, United States of America

^b Department of Neurology, McKnight Brain Institute, University of Florida, Gainesville FL 32611, United States of America

^c Department of Psychiatry, University of Florida, Gainesville FL 32611, United States of America

^d Department of Neuroscience, University of Florida, Gainesville FL 32611, United States of America

^e Center for Translational Research in Neurodegenerative Diseases, University of Florida, Gainesville FL 32611, United States of America

^f Wein Center for Alzheimer's Disease and Memory Disorders, Mount Sinai Medical Center, Miami Beach, FL 33140, United States of America

^g Center for Advanced Technology and Education, Florida International University, Miami, FL 33174, United States of America

^h Department of Neurology, University of Florida, Gainesville FL-32611, United States of America

ⁱ Department of Biomedical Engineering, University of Florida, Gainesville FL-32611, United States of America

^j College of Health Solutions, Arizona State University, Phoenix, AZ, United States of America

ARTICLE INFO

Keywords:

Mild cognitive impairment
Neurodegeneration
Free-water imaging
Hippocampus

ABSTRACT

Validating sensitive markers of hippocampal degeneration is fundamental for understanding neurodegenerative conditions such as Alzheimer's disease. In this paper, we test the hypothesis that free-water in the hippocampus will be more sensitive to early stages of cognitive decline than hippocampal volume, and that free-water in hippocampus will increase across distinct clinical stages of Alzheimer's disease. We examined two separate cohorts ($N = 126$; $N = 112$) of cognitively normal controls, early and late mild cognitive impairment (MCI), and Alzheimer's disease. Demographic, clinical, diffusion-weighted and T1-weighted imaging, and positron emission tomography (PET) imaging were assessed. Results indicated elevated hippocampal free-water in early MCI individuals compared to controls across both cohorts. In contrast, there was no difference in volume of these regions between controls and early MCI. ADNI free-water values in the hippocampus was associated with low CSF AB₁₋₄₂ levels and high global amyloid PET values. Free-water imaging of the hippocampus can serve as an early stage marker for AD and provides a complementary measure of AD neurodegeneration using non-invasive imaging.

1. Introduction

Alzheimer's disease (AD) is the most common cause of dementia in older adults, with increasing prevalence in individuals over 70 years of age. AD is characterized typically by memory impairment and neuropathological findings of beta amyloid plaques and neurofibrillary tangles (Braak and Braak, 1998). Although a definitive diagnosis currently cannot be made until autopsy, in-vivo biomarker development has emerged as a powerful tool to monitor disease progression and management (Jack Jr. et al., 2010; Jack et al., 1992) including structural

magnetic resonance imaging (MRI) techniques as a clinical tool to identify stages of early cognitive decline and AD (Doherty et al., 2015; Okonkwo et al., 2014).

The hippocampus undergoes atrophic and pathological changes prior to symptomatic onset (Janocko et al., 2012; Mueller and Weiner, 2009). The changes that occur in the hippocampus has even been documented to impact hippocampal sub-regions differentially (Frisoni et al., 2006) (Padurariu et al., 2012). Although these differences may be due to the methods of analysis, inclusion criteria, or type of MCI, these studies indicate that characterization of hippocampal degeneration is

* Corresponding author at: College of Health Solutions, Arizona State University, Phoenix, AZ 85004, United States of America.

E-mail address: edward.ofori@asu.edu (E. Ofori).

¹ Data used in preparation of this article were obtained from the Alzheimer's Disease Neuroimaging Initiative (ADNI) database (adni.loni.usc.edu). As such, the investigators within the ADNI contributed to the design and implementation of ADNI and/or provided data but did not participate in analysis or writing of this report. A complete listing of ADNI investigators can be found at: http://adni.loni.usc.edu/wp-content/uploads/how_to_apply/ADNI_Acknowledgement_List.pdf.

<https://doi.org/10.1016/j.nicl.2019.101985>

Received 25 February 2019; Received in revised form 30 June 2019; Accepted 14 August 2019

Available online 22 August 2019

2213-1582/ © 2019 Published by Elsevier Inc. This is an open access article under the CC BY-NC-ND license (<http://creativecommons.org/licenses/by-nc-nd/4.0/>).

important in stages of cognitive impairment and AD. Further, the pathological changes due to intraneuronal tau or extracellular accumulation of amyloid- β (A β) in the hippocampus lead to neuronal shrinkage (Lee et al., 2001), providing greater increase of the extracellular space.

Diffusion MRI studies have shown that individuals with MCI or AD have increased hippocampal mean diffusivity (Ashford et al., 2011; Clerx et al., 2012). Examining microstructural changes may be a more sensitive predictor of clinical decline than macrostructural volume measurements of the hippocampus. Recently, a new diffusion MRI technique, free water mapping, has been shown to assay extracellular space, detect neurodegeneration (Pasternak et al., 2009), and improve classification compared to single-tensor metrics (Ofori et al., 2017). In this study, we tested the hypothesis that free-water within the hippocampus would detect differences among various stages along the AD clinical continuum and correlate with clinical severity. We also examined the extent to which free-water measures of hippocampus correlated with other measures of AD pathophysiological processes. These analyses were carried out sequentially, in two large cohorts for rigorous validation of the findings.

2. Methods

2.1. Subjects

Imaging data for the current study were obtained from 2 databases: 1) the Alzheimer's Neuroimaging Initiative (ADNI) database and 2) the 1Florida Alzheimer's Disease Research Center (1Florida ADRC). ADNI has collected data through 3 phases and the ADNI data are from the ADNI 2 Phase. ADNI-2 data were used because data were collected from subjects at distinct stages of clinical severity. More details regarding the ADNI-2 protocol can be found at <https://adni.loni.usc.edu/wp-content/uploads/2008/07/adni2-procedures-manual.pdf>. The primary goal of ADNI has been to test whether serial MRI, positron emission tomography (PET), other blood and CSF markers, and clinical and neuropsychological assessment can be combined to measure the progression from the earliest mild cognitive impairment (MCI) through early Alzheimer's disease (AD). For up-to-date information, go to www.adni-info.org. ADNI Diagnostic criteria for each clinical stage was applied to 1Florida ADRC participants. The 1Florida ADRC data are from subjects enrolled at Mount Sinai Medical Center from October 19th, 2015 to December 1st, 2017. All subjects recruited were between ages 55–90. Briefly, subjects were divided into four groups in both ADNI and 1Florida ADRC groups: 26 (ADNI; baseline age: 72.8 ± 6.6 years) and 32 (1Florida ADRC; baseline 68.9 ± 6.4 years) cognitively normal elderly controls, 45 (ADNI; baseline age: 72.7 ± 8.0 years) and 33 (1Florida ADRC; baseline 70.8 ± 7.4 years) patients with EMCI, 26 ADNI LMCI (baseline age: 73.2 ± 6.0 years) and 22 1Florida ADRC LMCI (baseline age: 74.1 ± 7.6 years), and 29 ADNI patients with AD (baseline age: 73.9 ± 8.5 years) and 25 1Florida ADRC patients with AD (baseline age: 71.5 ± 10.2 years). All participants had assessments which included a Clinical Dementia Rating-Sum of Boxes (CDR-SB) (Coley et al., 2011; Morris, 1993), Mini-Mental State Exam (MMSE) (Folstein et al., 1975), Montreal Cognitive Assessment (MoCA) (Nasreddine et al., 2005), apolipoprotein (ApoE) $\epsilon 4$ status, diffusion MRI, T1 MRI, intracranial volume determination, and amyloid PET imaging data (18F-florbetapir for ADNI and 18F-florbetaben for 1Florida ADRC).

2.2. Data acquisition

The Search Criteria used to acquire data identified subjects from the initial or screening visit. The ADNI T1 scans were acquired with a Gradient recalled echo (GRE) pulse sequence with acquisition in the sagittal plane, repetition time (TR) of 6.98 ms, echo time (TE) of 2.85 ms, inversion time (TI) of 400 ms, 26 cm field of view, with a $256 \times 256 \times 196$ acquisition matrix in the x-, y-, and z-dimensions,

Table 1
Scanner information.

	ADNI		1FLORIDA ADRC	
Manufacturer	GE		SIEMENS	
Type	DIFF	T1	DIFF	T1
Directions	41	N/A	64	N/A
Sequence	EPSE	GRE	echo	MPRAGE
TE	67	2.85	98	3.03
TI	N/A	400 ms	N/A	700 ms
TR	11,000	6.98	9000	1380
Flip angle	90	N/A	0	9
Slices	59	196	64	176
FOV	35 cm	26 cm	250 mm	250 mm
resolution	$2.7 \times 2.7 \times 2.7$	$1 \times 1 \times 1.2$	$2 \times 2 \times 2$	$1 \times 1 \times 1$
b-value	1000	N/A	1000	N/A
# of b0	6	N/A	1	N/A

Abbreviations: DIFF = diffusion, EPSE = echo-planar spin-echo, FOV = field of view, GE = General Electric, GRE = gradient echo, MP-RAGE = magnetization prepared-rapid acquisition gradient echo, N/A = not available, TI = inversion time, TE = echo time, TR = repetition time.

yielding a voxel size of $1.0 \times 1.0 \times 1.2 \text{ mm}^3$. 1Florida ADRC T1 scans were acquired with using a 3 T Siemens Magnetom Skyra with a 20-channel head/neck coil with a Magnetization Prepared Rapid Gradient Echo (MPRAGE) pulse sequence with acquisition in the sagittal plane, TR of 1380 ms, TE of 3.03 ms, with a $250 \times 250 \times 176 \text{ mm}$ acquisition matrix in the x-, y-, and z-dimensions, yielding a voxel size of $1.0 \times 1.0 \times 1.0 \text{ mm}^3$ (See Table 2).

ADNI diffusion imaging scans were acquired with a 41 direction "EP/SE" pulse sequence b-value 1000 and 5 b0 images with a 2D acquisition, average TR of $\sim 11,000$ ms, average TE of 67 ms, flip angle of 90° , in-plane resolution = $2.7 \times 2.7 \text{ mm}$, slice number = 59, and slice thickness = 2.7 mm with no gap and 35 cm field of view. 1Florida ADRC diffusion imaging scans were acquired with a 64 direction echo planar sequence b-value 1000 with 1 b0 image with TR of 9000 ms, TE of 90 ms, flip angle of 90° , in-plane resolution = $2 \times 2 \text{ mm}$, slice number = 64, and a slice thickness of 2 mm with no gap (See Table 1). ADNI data were acquired from 12 different scanners and 1Florida ADRC data were acquired from 1 scanner.

The PET scanner currently used for the 1Florida ADRC has been certified for use in ADNI. A 3D Hoffmann brain phantom was acquired prior to participant enrollment in order to establish a standardized acquisition and reconstruction method. Participants were infused with [18-F] florbetaben 300 MBQ over a 3 min period. Scanning commenced after a period of 60 min for a duration of 20 min on a Siemens Biograph 16 PET/CT scanner, operating in 3D mode (55 slices/frame, 3 mm slice thickness 128×128 matrix). Acquired PET data were reconstructed into a $128 \times 128 \times 63$ (axial) matrix with voxel dimensions of $0.21 \times 0.21 \times 0.24 \text{ cm}$. Reconstruction was performed using manufacturer-supplied software and included corrections for attenuation, scatter, random coincidences and dead time. Images for regional analyses were processed using Fourier analysis followed by direct Fourier reconstruction. Images were smoothed with a 3 mm Hann filter. Following reconstruction, image sets were inspected and, if necessary, corrected for inter-frame motion.

2.3. Imaging processing

For each subject, all baseline raw diffusion weighted imaging (DWI) volumes were aligned with the FMRIB Software Library (FSL) eddy-correct tool (<http://www.fmrib.ox.ac.uk/fsl>) to correct for head motion and eddy-current distortions. Gradient directions were rotated based on motion corrections. All voxels outside of the brain and eye-tissue were subsequently removed from diffusion-weighted images using the Brain Extraction Tool from FSL. Free-water maps were calculated for all subjects; computational routines for free-water have been published

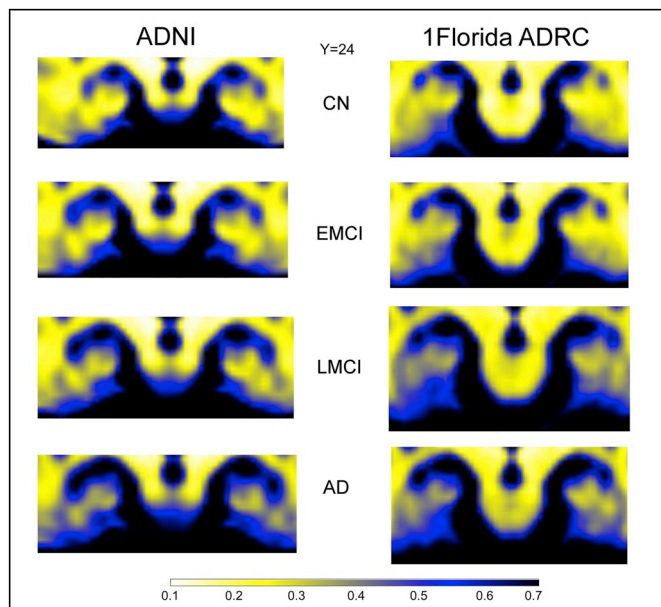


Fig. 1. Displays coronal sections of the group mean free-water maps at $y = 24$ in MNI space of the hippocampus for ADNI and 1Florida ADRC across cognitive normal (CN), early mild cognitive impairment (EMCI), late mild cognitive impairment (LMCI), and Alzheimer's disease (AD). White-yellowish colors indicate low free-water areas whereas blue-black colors indicate high free-water areas.

elsewhere (Ofori et al., 2015; Pasternak et al., 2009). All maps were warped into standardized space using ANTs R routines (Avants et al., 2008; Avants et al., 2014). First, a linear rigid transformation was performed. Then a diffeomorphic transformation using the Symmetric Normalization (SyN) transformation model was performed. SyN uses a gradient-based iterative convergence using diffeomorphisms to converge on an optimal solution based on a similarity metric (e.g., cross-correlation) (Klein et al., 2009). The diffeomorphic transform matrices were then applied to all the free-water maps, for subsequent analyses of hippocampal regions (Fig. 1).

2.3.1. Volumetric MRI analysis

Regional analysis was done on the 3D T1 MPRAGE imager with FreeSurfer (<http://surfer.nmr.mgh.harvard.edu/>) (Dale et al., 1999). This MRI software package is comprised of a suite of automated tools for segmentation, reconstruction, and derivation of regional volumes and surface-based rendering. FreeSurfer 6.0 was used to derive hippocampal volumes. We employed the same software version, workstation, and operating system throughout the study given known variability introduced by these factors.

2.3.2. PET imaging analysis

PET imaging data were downloaded from the ADNI website (<https://adni.loni.usc.edu>). Signal uptake value ratios (SUVRs) for amyloid-PET were calculated based on previously reported methods (Jagust et al., 2010). The PET tracer ^{18}F -florbetapir was used to quantify global amyloid status, calculated by ratios of regions of interest (ROIs) tracer retention to cerebellar and total white matter uptake. The cutoff SUVR value to determine subject status as "amyloid positive" was 1.1 using frontal lobe, anterior cingulate, precuneus, and parietal cortex relative to cerebellum. More details of the methods for the PET analyses can be found at <http://adni.loni.usc.edu/methods/pet-analysis/>.

Images were obtained from the top of the head to the top of the neck and CT data were employed for initial attenuation correction and image reconstruction in the sagittal, axial and coronal planes. The florbetaben PET/CT scans, including the outline of the skull, were co-registered

linearly (i.e., trilinear interpolation) with 12 degrees of freedom, onto the volumetric MRI scan using a T1-weighted, (magnetization prepared rapid gradient echo (MP-RAGE) sequence. Region-of-interest (ROI) boundaries were manually defined using the structural MRI for anatomical reference and criteria that have been proven to provide highly reproducible outcomes (Desikan et al., 2006). This registration process ensured that the florbetaben PET/CT image had the same accurate segmentation and parcellation as in the MRI. Atrophy correction was not used because the additional noise-error added to quantification of regional counts in the PET images.

Quantitative assessment of PET scans: Image processing was performed as previously described (Barthel et al., 2011). The average activity was calculated in the ROIs corresponding to cerebellar gray matter and cerebral cortical regions. A composite SUVR was calculated by the ratio of the mean SUVR of the 5 cortical regions (frontal, temporal, parietal, anterior and posterior cingulate cortex regions, each region summed from left and right hemispheres) and the cerebellar gray matter (Rowe et al., 2008).

2.4. APOE genotyping

Samples were genotyped for the APOE $\epsilon 2$, $\epsilon 3$ and $\epsilon 4$ alleles using pre-designed TaqMan SNP Genotyping Assays for SNPs rs7412 and rs429358 (Thermo Fisher Scientific, Massachusetts, USA) on the QuantStudio 7 Flex Real-Time PCR system (Applied Biosystems, California, USA) following the manufacturer's protocol. This genotyping allowed us to determine whether participants had $\epsilon 4$ positive or negative. The APOE $\epsilon 4$ allele has shown to occur in a higher prevalence in individuals with Alzheimer's disease than found the non-AD patients (Farrer et al., 1997).

2.5. CSF analysis

Baseline CSF samples were obtained in the morning after an overnight fast and processed as previously described (Shaw et al., 2009; Shaw et al., 2011). Briefly, CSF was collected into polypropylene collection tubes or syringes provided to each site, then transferred into polypropylene transfer tubes without any centrifugation step followed by freezing on dry ice within 1 h after collection, and shipped overnight to the ADNI Biomarker Core laboratory at the University of Pennsylvania Medical Center on dry ice. Aliquots (0.5 ml) were prepared from these samples after thawing (1 h) at room temperature and gentle mixing. The aliquots were stored in bar code-labeled polypropylene vials at -80°C . $\text{A}\beta_{1-42}$, t-tau, and p-tau $_{181}$ were measured using the multiplex xMAP Luminex platform (Luminex Corp, Austin, TX) with Innogenetics (INNO-BIA AlzBio3; Ghent, Belgium; for research use-only reagents) immunoassay kit-based reagents.

2.6. Region of interest analyses

ROI analyses were performed utilizing the segmented hippocampal masks that were obtained through FreeSurfer 6.0. Data from both the left and right hemispheres were obtained. These individual voxels within a ROI were then pooled together to get an average for either the left or right hippocampal region.

2.7. Statistical analyses

Measures of age, years of education, CDR-SB, MMSE, MoCA, and ICV were compared using one-way ANOVAs across the groups. Post-hoc tests of means were evaluated using the Tukey's HSD procedure. In order to detect differences between sites, we ran a MANCOVA on continuous demographic variables with site as a covariate. Differences in sex, amyloid status (positive or negative), and ApoE4 carrier status were assessed with Chi-square analyses separate for each site. Mean values for the hippocampal ROIs were calculated for free-water and

hippocampal volume. MANCOVAs were calculated, controlling for sex, age, education, site and ApoE e4 status, with group status as the fixed factor. Post-hoc tests for the group status were evaluated using Bonferroni pairwise comparisons. Statistical threshold was set at $p < .05$.

2.8. Correlational analyses

Spearman rho (ρ) statistic was employed for correlations between dependent free-water values and MOCA, MMSE, CSF measures and global amyloid. The Spearman rho correlations can provide information to the degree hippocampus free-water levels are associated with clinical measures along with CSF. The determination of this relationship can help further develop prediction models with longitudinal data. P -values were corrected for multiple comparisons controlling for false discovery rate (FDR) (Benjamini and Hochberg, 1995).

3. Results

3.1. Demographics and clinical data

There were no significant differences (p -values $> .05$) among diagnostic groups for age, sex, ICV and years of education (Table 2) for either the ADNI or 1Florida ADRC cohorts. As expected, there were significant differences among groups for CDR-SB, MMSE and MoCA, scores (p -values $< .05$) across both cohorts. The number of amyloid positive individuals were different among groups (p -values $< .05$). For ADNI, there were more amyloid positive and ApoE e4 carriers in the LMCI and AD groups than there were in EMCI and CN (p -values $< .01$). For 1Florida ADRC there were more amyloid positive carriers in the AD than EMCI and LMCI groups, and more positive carriers in the EMCI and LMCI than CN.

In the ADNI cohort, post-hoc tests revealed lower CDR-SB scores for controls compared to EMCI and LMCI; the AD group had the highest CDR-SB scores (see Table 2). Post hoc testing revealed the following pattern of results for MoCA: CN $>$ EMCI $>$ LMCI $>$ AD. MMSE scores were lower for the AD group than the CN, EMCI, and LMCI groups, and higher (better) in the CN and EMCI groups than in the LMCI and AD groups (p -values $< .01$; see Table 2).

For the 1Florida ADRC cohort, post-hoc tests revealed lower CDR-SB scores for controls and EMCI when compared with LMCI and AD (see Table 2). Post hoc testing revealed that AD MoCA scores were

Table 2 Demographic and clinical information.

	ADNI					Statistics	1Florida ADRC					Statistics
	CN	EMCI	LMCI	AD	CN		EMCI	LMCI	AD			
N	26	45	26	29	-	29	29	25	29	-		
Age	72.8 (6.6)	72.7 (8.0)	73.2 (6.0)	73.9 (8.5)	$F = 0.17, p = .92$	67.9 (10.0)	72.8 (7.2)	73.6 (7.4)	72.2 (9.6)	$F = 2.4, p = .07$		
Sex (M/F)	12/14	30/15	17/9	16/13	$\chi^2 = 3.5, p = .32$	10/19	10/19	14/11	16/13	$\chi^2 = 4.7, p = .19$		
Years of Education	16.5 (2.6)	16.0 (2.6)	15.5 (2.8)	14.7 (2.9)	$F = 2.3, p = .08$	16.2 (3.1)	15.4 (3.5)	14.7 (3.3)	14.0 (4.1)	$F = 2.05, p = .11$		
CDR-SB	0.02 (0.09)	1.2 (0.7)	1.6 (0.9)	4.7 (1.4)	$F = 143.2, p = 8.5E-40$	0.3 (0.9)	0.9 (0.4)	2.9 (0.9)	6.7 (3.3)	$F = 76.3, p = 9.4E-27$		
MMSE	28.8 (1.4)	28.0 (1.6)	27.4 (2.0)	23.6 (2.0)	$F = 51.3, p = 1.6E-21$	29.1 (1.0)	27.7 (2.4)	25.7 (2.7)	21.4 (5.9)	$F = 1.6, p = 4.2E-12$		
MoCA	26.2 (2.4)	23.6 (2.4)	21.6 (2.3)	17.8 (4.7)	$F = 37.2, p = 4.0E-17$	24.9 (2.8)	23.0 (3.1)	22.2 (10.1)	14.2 (6.3)	$F = 14.57, p = 7.0E-8$		
Amyloid Status (-/+)	24/0	23/18	6/18	4/25	$\chi^2 = 41.8, p = 4.5E-9$	25/0	16/6	13/9	7/15	$\chi^2 = 25.6, p = .0002$		
ApoE e4 Carriers (0/1+)	18/7	28/16	5/20	9/19	$\chi^2 = 20.7, p = .0001$	20/6	21/8	10/13	19/7	$\chi^2 = 7.8, p = .05$		
Intracranial Volume (L)	1.41 (0.14)	1.49 (0.14)	1.48 (0.12)	1.42 (0.16)	$F = 2.0, p = .116$	1.34 (0.13)	1.36 (0.17)	1.40 (0.18)	1.42 (0.21)	$F = 1.36, p = .26$		

Data are either count or mean (\pm SD). Abbreviations: AD = Alzheimer's disease, ApoE = apolipoprotein, CDR-SB = clinical dementia rating- sum of boxes, CN = Cognitively Normal, EMCI = Early Mild Cognitive Impairment, F = female, ICV = Intracranial Volume, L = Liters, LMCI = Late Mild Cognitive Impairment, M = male, MMSE = Mini-Mental State Examination, MoCA = Montreal Cognitive Assessment.

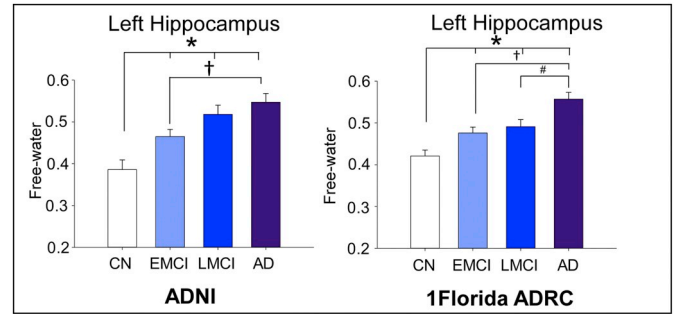


Fig. 2. Displays bar-graphs of free-water levels for the left and right hippocampus in CN, EMCI, LMCI, and AD patients. The asterisk indicates significant differences between CN, EMCI, LMCI, and AD. The cross indicates significant differences between EMCI and AD. The pound sign indicates significant differences between LMCI and AD.

significantly lower than CN, EMCI and LMCI groups. MMSE scores decreased with increases in disease severity with CN having the highest scores and AD having the lowest scores (p -values $< .01$; see Table 2).

Statistical analyses also revealed the influence of the site covariate on the continuous demographic variables. We found no site effect for age ($F = 0, p = .98$), MoCA ($F = 2.6, p = .11$), MMSE ($F = 2.7, p = .11$). There was a significant effect for years of education with the ADNI site have more years of education than the 1Florida ADRC site ($F = 14.3, p = 2E-4$) and CDR-SB ($F = 14.2, p = 1.9E-4$) which resulted in greater scores in the 1Florida ADRC cohort.

3.2. Diffusion analyses

Fig. 2A illustrates the group free-water in MNI space at $y = 24$, and Fig. 2B shows the bar plots for free-water in each cohort for left hippocampus. Significant effects were found for mean free-water values in both hippocampal ROIs (F 's $> 2.5, p$ -values $< .01$) (See Fig. 2). The left hippocampal ROI ($F = 16.35, p = 1.5E-9$) revealed increased free-water values for the AD group (0.56), LMCI group (0.51) and EMCI group (0.48) when compared to CN (0.42, p -values $< .003$). EMCI group free-water values were also lower than the AD group ($p = 2E-4$). This pattern of findings was found to be consistent when both cohorts were analyzed separately ($p < 1E-5$). The right hippocampal ($F = 3.2, p = .023$) revealed increased free-water for AD (0.50) when compared

to CN (0.43), with no significant differences in free-water levels between the EMCI group (0.47) and the LMCI group (0.49).

Statistical analyses revealed a significant covariate of age ($F = 24.51$, $p = 2E-6$) and site ($F = 8.5$, $p = .004$) on the left hemisphere free-water values, whereas there were significant covariate effects of age and sex for the right hemisphere free-water values (F 's > 2 , p -values $> .05$). There were no significant covariate effects for education, ApoE $\epsilon 4$ on either dependent variable (F 's > 2 , p -values $> .05$). The age covariate in the model showed a positive intercept indicated increases in free-water with age for the left-hemisphere free-water values. The site covariate resulted in higher values in the 1Florida ADRC cohort than the ADNI cohort. As noted above, this did not change the pattern of findings for either cohort. For the right hippocampal free-water values, age covariate ($F = 6.5$, $p = .012$) results in increases in free-water and sex covariate ($F = 6.5$, $p = .012$) results in decreases in free-water.

3.3. Volumetric analyses

For the ADNI cohort, a significant group effect was found for all left and right hippocampal ROIs (F 's > 9 , $FDR p < .01$). Post hoc analysis revealed no significant differences between the CN and EMCI groups for any hippocampal ROIs (F 's > 9 , p 's > 0.05). The left hippocampus ($F = 24.4$, $p = 2.4E-12$) volumes were significantly lower for the AD and LMCI groups when compared to the CN and EMCI groups. Right hippocampal ($F = 26.9$, $p = 2.4E-13$) showed a similar pattern of results as their left counterparts, in addition volumes for the AD group were lower than the LMCI group whereas the left side did not show a difference between these two groups.

For the 1Florida ADRC cohort, a significant group effect was also found for all left and right hippocampal volumes similar to the ADNI findings (F 's > 9 , p 's < 0.01). The left hippocampus ($F = 9.0$, $p = 2.2E-5$) volumes were significantly lower for the AD group when compared to controls and EMCI groups. The right hippocampal ($F = 10.7$, $p = 4E-6$) volumes were significantly lower for the AD group when compared to controls, EMCI and LMCI groups. There were no significant covariate effects of site, education, ApoE $\epsilon 4$ status on volumetric measures. There was a significant effect of age on hippocampal volumetric measures. The age covariate indicates decreases in volume with increases in age.

3.4. Correlation analyses

Free-water values from both hippocampal ROIs were correlated with MMSE and MoCA (Table 3). Significant negative associations were found among all ROIs with MMSE and MoCA.

Correlations between free-water measures and amyloid PET data revealed several significant relationships. All regions were found to positively correlate with AV45 with the left hippocampal free-water levels demonstrating the greatest correlation among ROIs.

Correlational analyses between CSF measures and free-water levels revealed several significant correlations. For free-water, left and right hippocampus regions were found to moderately correlate inversely

with CSF AB₁₋₄₂ levels. There were no significant correlations between free-water levels and p-tau or t-tau ($p > .05$) (See Table 3).

4. Discussion

The current investigation examined the integrity of hippocampal regions by assessing free-water imaging in different stages of AD across ADNI and the 1Florida ADRC. The results indicate that left hippocampal free-water values were elevated in EMCI when compared to CN, across both the ADNI and 1Florida ADRC cohorts. ADNI free-water measures from both hemispheres correlated with clinical cognition scores. In addition, free-water values were associated with global AV45 and CSF AB₁₋₄₂ levels and not CSF p-tau and CSF t-tau, suggesting free-water may provide specific information about the pathological process in AD. Thus, the current study suggests that free-water mapping of bilateral hippocampus provides important information of neurodegenerative changes in AD.

Previous studies have shown that elevated mean diffusivity (MD) in the hippocampus is a precursor to symptomatic AD and can detect early stage changes of AD (Fellgiebel and Yakushev, 2011). It has been suggested that this elevation in MD is due to increased extracellular water content or decreased gray matter density (Fellgiebel and Yakushev, 2011). Our findings extend previous work suggesting diffusion metrics are elevated in the hippocampus, and that they are more sensitive to hippocampal change than volumetric imaging. It is important to note that we used Freesurfer 6.0 which has improved segmentation for volume, and free-water remained more sensitive to left hippocampal change in early MCI for both cohorts. Although, we found increases in left and right free-water measures from the hippocampus between CN and EMCI, in both ADNI and ADRC cohorts, volumetric measures between CN and EMCI revealed no detectable changes in these same regions. The current results suggest that changes occurring early in the AD pathophysiological process may relate to microstructural changes in the left hippocampus. Coincidentally, there were inverse correlations between free-water levels in bilateral hippocampus and CSF AB₁₋₄₂ levels; whereas free-water levels were not associated with CSF total tau. Further, higher levels of free-water were associated with lower scores on the MMSE and the MoCA. These findings support the hypothesis that increased levels of free water in these hippocampal ROIs have functional and clinical relevance in the AD process, and may be among the earliest detectable structural changes. Pyramidal neuron loss within the hippocampus results in the connections to disconnect from their projection areas in the cortex (Davies et al., 1992; Padurariu et al., 2012). In a previous MRI study, it was reported that the greatest atrophy in the hippocampus occurred shows a systematic decline within the region (Frisoni et al., 2006). Nonetheless, the current study using diffusion imaging showed the hippocampal free-water values were elevated in EMCI patients. Free-water is suggested to estimate the size of the extracellular space and reflect the degenerative processes that occur in this area. There is some support for the hypothesis that the changes seen within these particular hippocampal regions are due to cholinergic and glutamatergic terminal loss from the nucleus basalis and lamina II of the entorhinal cortex (ERC) respectively (Kordower et al., 2001). In a

Table 3
Correlational analyses of free-water, CSF, PET imaging, and clinical measures.

	MMSE		MoCA		AV45		CSF A β ₁₋₄₂		CSF p-tau		CSF t-tau	
	ρ	FDR P-value	ρ	FDR P-value	ρ	FDR P-value	ρ	FDR P-value	ρ	FDR P-value	ρ	FDR P-value
Left Hippocampus Free-water	-0.45*	8.90E-06	-0.38*	0.005	0.30*	8.60E-03	-0.28*	0.004	0.09	0.47	0.21	0.06
Right Hippocampus Free-water	-0.42*	8.60E-06	-0.42*	3.45E-04	0.27*	0.003	-0.27*	0.008	0.11	0.36	0.13	0.27

The correlation coefficients and the corresponding p value are listed for each association, *indicates significant correlations ($FDR p < .05$). Abbreviations: A β = amyloid beta, AV45 = florbetapir, CSF = cerebrospinal fluid, MMSE = Mini-Mental State Examination, MoCA = Montreal Cognitive Assessment, p-tau = phosphorylated tau, and t-tau = total tau.

previous study demonstrated densities of choline acetyltransferase-positive punctate immunoprecipitates were found to be significantly higher in hippocampal areas for AD (Ransmayr et al., 1992) and that the neurofibrillary pathology first affects lamina II ERC neurons (Braak and Braak, 1991). The loss of cholinergic modulation in AD may contribute to a decline in memory.

Previous studies have shown correlations between cognitive measures and volumetric measures of hippocampus (Lim et al., 2012). The current study shows significant correlations between free-water from all hippocampal ROIs and various cognitive assessment scores. Our findings also support the hypothesis that MRI markers of cognitive impairment follow closely with clinical symptoms (Fellgiebel et al., 2004). This is consistent with prior findings that demonstrate correlations between hippocampal MD and F DG-PET (Aparicio et al., 2016). This may provide potential information to determine whether free-water may be used as a progression marker for AD and MCI. Although longitudinal confirmation would be required, if these findings are confirmed, they may provide a sensitive marker of the effects of therapeutic intervention, similar to the proposed use of free-water in Parkinson's disease (Burciu et al. 2017). Postmortem studies demonstrate accumulation of intraneuronal tau in the hippocampus from midlife onward (Braak and Braak, 1998). This is associated with inflammatory reactions and neuronal atrophy, and potentially larger amounts of extracellular fluid—which in turn may relate to higher free-water content.

We note three limitations that could influence the reported results. One, site differences between the cohorts could confound some of the reported results. We did covary for site to minimize this influence however as noted above the influence of site on some demographic and imaging variables requires further study. Further, more comprehensive neuropsychological test data would aid in characterization of the patient status. Finally, baseline data were only included and longitudinal data would help confirm the extent diagnoses, hippocampal imaging findings and potential changes in diagnoses are influenced by cross-sectional differences in the hippocampal free-water.

The current study found free-water levels were positively associated with global levels of AV45 and negatively associated with CSF A β 42, which correlates negatively with amyloid deposition in the brain (Kang et al., 2013; Verbeek et al., 2009). However, free-water levels did not correlate with CSF p-tau or CSF t-tau in our study, suggesting the possibility that the increase in free water levels may reflect amyloid-induced prodromal neurodegenerative changes in the hippocampus occurring prior to the increase in CSF tau. This hypothesis is supported by the known time course of events, which have been validated in longitudinal studies, showing that increases in brain amyloid levels precede increases in CSF tau by a decade or more (Jack et al., 2010). In summary, our study suggests that free-water values from the hippocampus may reflect a pathophysiological process along the entire AD continuum, in the presence of increased global amyloid deposition, but prior to overt evidence of neurodegeneration in the form of hippocampal atrophy or increased CSF tau increases. We found evidence that hippocampal free-water values served as a very early marker of cognitive impairment with changes detected in EMCI, in two separate large cohorts. We suggest that hippocampal free-water levels provide distinct and sensitive in-vivo information about AD neurodegeneration.

Author disclosures

Dr. Ofori reports no disclosures. Dr. DeKosky serves as a consultation for Amgen, Acumen Pharmaceuticals, Biogen, and Cognition Therapeutics. Dr. Febo reports no disclosures. Dr. Colon-Perez reports no disclosures. Dr. Chakrabarty reports no disclosures. Dr. Duara receives grant support from Alzheimer's Therapeutic Research Institute, Avid-Eli Lilly & Company, Janssen Research & Development LLC, Merck & Company, Toyama Chemical Co., Ltd., and vTv Therapeutics LLC. Dr. Duara also serves as a consultant for Medical Learning Group. Dr. Adjouadi reports no disclosures. Dr. Golde receives grant support from

NIH, Michael J. Fox Foundation, Ellison Medical Foundation, and Thome Foundation. Dr. Vaillancourt receives grant support from NIH, NSF, and Tyler's Hope Foundation, and is co-founder and manager of Neuroimaging Solutions, LLC.

Funding sources

This study was supported by the 1Florida ADRC (P50AG047266), ADNI, and R01 NS052318.

Acknowledgements

Data used in the preparation of this article were obtained from the ADNI database (www.loni.ucla.edu/ADNI).

Data collection and sharing for this project was funded by the Alzheimer's Disease Neuroimaging Initiative (ADNI) (National Institutes of Health Grant U01 AG024904) and DOD ADNI (Department of Defense award number W81XWH-12-2-0012). ADNI is funded by the National Institute on Aging, the National Institute of Biomedical Imaging and Bioengineering, and through generous contributions from the following: AbbVie, Alzheimer's Association; Alzheimer's Drug Discovery Foundation; Araclon Biotech; BioClinica, Inc.; Biogen; Bristol-Myers Squibb Company; CereSpir, Inc.; Cogstate; Eisai Inc.; Elan Pharmaceuticals, Inc.; Eli Lilly and Company; EuroImmun; F. Hoffmann-La Roche Ltd. and its affiliated company Genentech, Inc.; Fujirebio; GE Healthcare; IXICO Ltd.; Janssen Alzheimer Immunotherapy Research & Development, LLC.; Johnson & Johnson Pharmaceutical Research & Development LLC.; Lumosity; Lundbeck; Merck & Co., Inc.; Meso Scale Diagnostics, LLC.; NeuroRx Research; Neurotrack Technologies; Novartis Pharmaceuticals Corporation; Pfizer Inc.; Piramal Imaging; Servier; Takeda Pharmaceutical Company; and Transition Therapeutics. The Canadian Institutes of Health Research is providing funds to support ADNI clinical sites in Canada. Private sector contributions are facilitated by the Foundation for the National Institutes of Health (www.fnih.org). The grantee organization is the Northern California Institute for Research and Education, and the study is coordinated by the Alzheimer's Therapeutic Research Institute at the University of Southern California. ADNI data are disseminated by the Laboratory for Neuro Imaging at the University of Southern California.

References

- Aparicio, J., Carreño, M., Bargalló, N., Setoain, X., Rubí, S., Rumià, J., Falcón, C., Calvo, A., Martí-Fuster, B., Padilla, N., Boget, T., Pintor, L., Donaire, A., 2016. Combined (18)F-FDG-PET and diffusion tensor imaging in mesial temporal lobe epilepsy with hippocampal sclerosis. *NeuroImage* 12, 976–989.
- Ashford, J.W., Rosen, A., Adamson, M., Bayley, P., Sabri, O., Furst, A., Black, S.E., Weiner, M., Fellgiebel, A., Yakushev, I., 2011. Diffusion tensor imaging of the hippocampus in MCI and early Alzheimer's disease. *J. Alzheimers Dis.* 26, 257–262.
- Avants, B.B., Epstein, C.L., Grossman, M., Gee, J.C., 2008. Symmetric diffeomorphic image registration with cross-correlation: evaluating automated labeling of elderly and neurodegenerative brain. *Med. Image Anal.* 12 (1), 26–41.
- Avants, B.B., Tustison, N.J., Stauffer, M., Song, G., Wu, B., Gee, J.C., 2014. The insight Toolkit image registration framework. *Front. Neuroinformat.* 8, 44.
- Barthel, H., Luthardt, J., Becker, G., Patt, M., Hammerstein, E., Hartwig, K., Eggers, B., Sattler, B., Schildan, A., Hesse, S., Meyer, P.M., Wolf, H., Zimmermann, T., Reischl, J., Rohde, B., Gertz, H.J., Reininger, C., Sabri, O., 2011. Individualized quantification of brain beta-amyloid burden: results of a proof of mechanism phase 0 florbetaben PET trial in patients with Alzheimer's disease and healthy controls. *Eur. J. Nucl. Med. Mol. imaging* 38 (9), 1702–1714.
- Benjamini, Y., Hochberg, Y., 1995. Controlling the false discovery rate: a practical and powerful approach to multiple testing. *J. R. Stat. Soc. Ser. B Methodol.* 57 (1), 289–300.
- Braak, H., Braak, E., 1991. Neuropathological staging of Alzheimer-related changes. *Acta Neuropathol.* 82 (4), 239–259.
- Braak, H., Braak, E., 1998. Evolution of neuronal changes in the course of Alzheimer's disease. *J. Neural Transm. Suppl.* 53.
- Burciu, R.G., Ofori, E., Archer, D.B., Wu, S.S., Pasternak, O., McFarland, N.R., Okun, M.S., Vaillancourt, D.E., 2017. Progression marker of Parkinson's disease: a 4-year multi-site imaging study. *Brain : J. Neurol.* 140 (8), 2183–2192.
- Clerx, L., Visser, P.J., Verhey, F., Aalten, P., 2012. New MRI markers for Alzheimer's disease: a meta-analysis of diffusion tensor imaging and a comparison with medial temporal lobe measurements. *J. Alzheimers Dis.* 29 (2), 405–429.

- Coley, N., Andrieu, S., Jaros, M., Weiner, M., Cedarbaum, J., Vellas, B., 2011. Suitability of the clinical dementia rating-sum of boxes as a single primary endpoint for Alzheimer's disease trials. *Alzheimers Dement.* 7 (6) (602-610.e602).
- Dale, A.M., Fischl, B., Sereno, M.I., 1999. Cortical surface-based analysis. I. Segmentation and surface reconstruction. *Neuroimage* 9 (2), 179-194.
- Davies, D.C., Horwood, N., Isaacs, S.L., Mann, D.M.A., 1992. The effect of age and Alzheimer's-disease on pyramidal neuron density in the individual fields of the hippocampal-formation. *Acta Neuropathol.* 83 (5), 510-517.
- Desikan, R.S., Segonne, F., Fischl, B., Quinn, B.T., Dickerson, B.C., Blacker, D., Buckner, R.L., Dale, A.M., Maguire, R.P., Hyman, B.T., Albert, M.S., Killiany, R.J., 2006. An automated labeling system for subdividing the human cerebral cortex on MRI scans into gyral based regions of interest. *Neuroimage* 31 (3), 968-980.
- Doherty, B.M., Schultz, S.A., Oh, J.M., Kosciak, R.L., Dowling, N.M., Barnhart, T.E., Murali, D., Gallagher, C.L., Carlsson, C.M., Bendlin, B.B., LaRue, A., Hermann, B.P., Rowley, H.A., Asthana, S., Sager, M.A., Christian, B.T., Johnson, S.C., Okonkwo, O.C., 2015. Amyloid burden, cortical thickness, and cognitive function in the Wisconsin Registry for Alzheimer's Prevention. *Alzheimers Dement.* 1 (2), 160-169.
- Farrer, L.A., Cupples, L.A., Haines, J.L., Hyman, B., Kukull, W.A., Mayeux, R., Myers, R.H., Pericak-Vance, M.A., Risch, N., van Duijn, C.M., 1997. Effects of age, sex, and ethnicity on the association between apolipoprotein E genotype and Alzheimer disease. A meta-analysis. APOE and Alzheimer Disease Meta Analysis Consortium. *JAMA* 278 (16), 1349-1356.
- Fellgiebel, A., Yakushev, I., 2011. Diffusion tensor imaging of the hippocampus in MCI and early Alzheimer's disease. *J. Alzheimers Dis.* 26 (Suppl. 3), 257-262.
- Fellgiebel, A., Wille, P., Muller, M.J., Winterer, G., Scheurich, A., Vucurevic, G., Schmidt, L.G., Stoeter, P., 2004. Ultrastructural hippocampal and white matter alterations in mild cognitive impairment: a diffusion tensor imaging study. *Dement. Geriatr. Cogn. Disord.* 18 (1), 101-108.
- Folstein, M.F., Folstein, S.E., McHugh, P.R., 1975. Mini-mental state. A practical method for grading the cognitive state of patients for the clinician. *J. Psychiatr. Res.* 12 (3), 189-198.
- Frisoni, G.B., Sabatelli, F., Lee, A.D., Dutton, R.A., Toga, A.W., Thompson, P.M., 2006. In vivo neuropathology of the hippocampal formation in AD: a radial mapping MR-based study. *NeuroImage* 32 (1), 104-110.
- Jack Jr., C.R., Knopman, D.S., Jagust, W.J., Shaw, L.M., Aisen, P.S., Weiner, M.W., Petersen, R.C., Trojanowski, J.Q., 2010. Hypothetical model of dynamic biomarkers of the Alzheimer's pathological cascade. *Lancet Neurol.* 9 (1), 119-128.
- Jack, C.R., Petersen, R.C., O'Brien, P.C., Tangalos, E.G., 1992. MR-based hippocampal volumetry in the diagnosis of Alzheimer's disease. *Neurology* 42.
- Jagust, W.J., Bandy, D., Chen, K., Foster, N.L., Landau, S.M., Mathis, C.A., Price, J.C., Reiman, E.M., Skovronsky, D., Koeppe, R.A., Investigators, A., 2010. The ADNI PET Core. *Alzheimers Dement.* 6 (3), 221-229.
- Janocko, N.J., Brodersen, K.A., Soto-Ortolaza, A.I., Ross, O.A., Liesinger, A.M., Duara, R., Graff-Radford, N.R., Dickson, D.W., Murray, M.E., 2012. Neuropathologically defined subtypes of Alzheimer's disease differ significantly from neurofibrillary tangle-predominant dementia. *Acta Neuropathol.* 124 (5), 681-692.
- Kang, J.H., Korecka, M., Toledo, J.B., Trojanowski, J.Q., Shaw, L.M., 2013. Clinical utility and analytical challenges in measurement of cerebrospinal fluid amyloid-beta(1-42) and tau proteins as Alzheimer disease biomarkers. *Clin. Chem.* 59 (6), 903-916.
- Klein, A., Andersson, J., Ardekani, B.A., Ashburner, J., Avants, B., Chiang, M.-C., Christensen, G.E., Collins, D.L., Gee, J., Hellier, P., Song, J.H., Jenkinson, M., Lepage, C., Rueckert, D., Thompson, P., Vercauteren, T., Woods, R.P., Mann, J.J., Parsey, R.V., 2009. Evaluation of 14 nonlinear deformation algorithms applied to human brain MRI registration. *NeuroImage* 46 (3), 786-802.
- Kordower, J.H., Chu, Y., Stebbins, G.T., DeKosky, S.T., Cochran, E.J., Bennett, D., Mufson, E.J., 2001. Loss and atrophy of layer II entorhinal cortex neurons in elderly people with mild cognitive impairment. *Ann. Neurol.* 49 (2), 202-213.
- Lee, V.M., Goedert, M., Trojanowski, J.Q., 2001. Neurodegenerative tauopathies. *Annu. Rev. Neurosci.* 24, 1121-1159.
- Lim, H.K., Jung, W.S., Ahn, K.J., Won, W.Y., Hahn, C., Lee, S.Y., Kim, I., Lee, C.U., 2012. Relationships between hippocampal shape and cognitive performances in drug-naïve patients with Alzheimer's disease. *Neurosci. Lett.* 516 (1), 124-129.
- Morris, J.C., 1993. The clinical dementia rating (CDR): current version and scoring rules. *Neurology* 43 (11), 2412-2414.
- Mueller, S.G., Weiner, M.W., 2009. Selective effect of age, Apo e4, and Alzheimer's disease on hippocampal subfields. *Hippocampus* 19 (6), 558-564.
- Nasreddine, Z.S., Phillips, N.A., Bedirian, V., Charbonneau, S., Whitehead, V., Collin, I., Cummings, J.L., Chertkow, H., 2005. The Montreal cognitive assessment, MoCA: a brief screening tool for mild cognitive impairment. *J. Am. Geriatr. Soc.* 53 (4), 695-699.
- Ofori, E., Pasternak, O., Planetta, P.J., Burciu, R., Snyder, A., Febo, M., Golde, T.E., Okun, M.S., Vaillancourt, D.E., 2015. Increased free water in the substantia nigra of Parkinson's disease: a single-site and multi-site study. *Neurobiol. Aging* 36 (2), 1097-1104.
- Ofori, E., Krismer, F., Burciu, R.G., Pasternak, O., McCracken, J.L., Lewis, M.M., Du, G., McFarland, N.R., Okun, M.S., Poewe, W., Mueller, C., Gizewski, E.R., Schocke, M., Kremser, C., Li, H., Huang, X., Seppi, K., Vaillancourt, D.E., 2017. Free water improves detection of changes in the substantia nigra in parkinsonism: a multisite study. *Mov. Disord.* 32 (10), 1457-1464.
- Okonkwo, O.C., Oh, J.M., Kosciak, R., Jonaitis, E., Cleary, C.A., Dowling, N.M., Bendlin, B.B., Larue, A., Hermann, B.P., Barnhart, T.E., Murali, D., Rowley, H.A., Carlsson, C.M., Gallagher, C.L., Asthana, S., Sager, M.A., Christian, B.T., Johnson, S.C., 2014. Amyloid burden, neuronal function, and cognitive decline in middle-aged adults at risk for Alzheimer's disease. *J. Int. Neuropsychol. Soc.* 20 (4), 422-433.
- Padurariu, M., Ciobica, A., Mavroudis, I., Fotiou, D., Baloyannis, S., 2012. Hippocampal neuronal loss in the CA1 and CA3 areas of Alzheimer's disease patients. *Psychiatr. Danub.* 24 (2), 152-158.
- Pasternak, O., Sochen, N., Gur, Y., Intrator, N., Assaf, Y., 2009. Free water elimination and mapping from diffusion MRI. *Magn. Reson. Med.* 62 (3), 717-730.
- Ransmayr, G., Cervera, P., Hirsch, E.C., Berger, W., Fischer, W., Agid, Y., 1992. Alzheimer's disease: is the decrease of the cholinergic innervation of the hippocampus related to intrinsic hippocampal pathology? *Neuroscience* 47 (4), 843-851.
- Rowe, C.C., Ackerman, U., Browne, W., Mulligan, R., Pike, K.L., 2008. Imaging of amyloid beta in Alzheimer's disease with 18F-BAY94-9172, a novel PET tracer: proof of mechanism. *Lancet. Neurol.* 7 (2), 129-135.
- Shaw, L.M., Vanderstichele, H., Knapiak-Czajka, M., Clark, C.M., Aisen, P.S., Petersen, R.C., Blennow, K., Soares, H., Simon, A., Lewczuk, P., Dean, R., Siemers, E., Potter, W., Lee, V.M.Y., Trojanowski, J.Q., 2009. Cerebrospinal fluid biomarker signature in Alzheimer's disease neuroimaging initiative subjects. *Ann. Neurol.* 65 (4), 403-413.
- Shaw, L.M., Vanderstichele, H., Knapiak-Czajka, M., Figurski, M., Coart, E., Blennow, K., Soares, H., Simon, A.J., Lewczuk, P., Dean, R.A., Siemers, E., Potter, W., Lee, V.M.Y., Trojanowski, J.Q., Alzheimer's Disease Neuroimaging, I., 2011. Qualification of the analytical and clinical performance of CSF biomarker analyses in ADNI. *Acta Neuropathol.* 121 (5), 597-609.
- Verbeek, M.M., Kremer, B.P.H., Rikkert, M.O., van Domburg, P.H.M.F., Skehan, M.E., Greenberg, S.M., 2009. Cerebrospinal fluid amyloid $\beta(40)$ is decreased in cerebral amyloid Angiopathy. *Ann. Neurol.* 66 (2), 245-249.